Studies on Blends of High-Density Polyethylene and Polypropylene Produced by Oscillating Shear Stress Field

Gong Zhang, Qiang Fu, Kaizhi Shen, Long Jian, Yong Wang

College of Polymer Science and Engineering, Sichuan University, State Key Laboratory of Polymer Materials Engineering, Chengdu 610065, People's Republic of China

ABSTRACT: Tensile strength and morphology of blends of high-density polyethylene (HDPE) and polypropylene (PP) obtained by oscillating packing injection molding were investigated via Universal Testing Machine, DSC, and SAXS. Tensile strength is greatly enhanced from 24.5 MPa to more than 90 MPa for pure HDPE and for blends with PP content less than 10 wt %. There exists a sharp decrease of tensile strength when PP content is more than 10 wt %. The shear-induced morphologies with core in the center, oriented zone surrounding the core and skin layer are observed in the cross-section areas of the samples. Interestingly, a sharp decrease of oriented zone is seen when PP content is more than 10 wt %, associated with the sharp decrease of tensile strength. DSC result shows double melting peaks with a high-temperature melting peak that is not present in the endotherm obtained from the central core and obtained from the samples by static packing injection molding, which indicates the existence of shish-kebab structure in the oriented zone. However, there is no difference of crystallinity between the samples by oscillating and by static packing injection molding. SAXS was used to analyze the complicated morphologies induced by shear stress, and results show that the crystal thickness could be greatly increased under shear stress. © 2002 Wiley Periodicals, Inc. J Appl Polym Sci 86: 58–63, 2002

Key words: polyethylene (PE); poly(propylene) (PP); blends; shear; morphology

INTRODUCTION

Study of the property and morphology of polyolefin blends has always received great interests, not only because of their widely application in industry, but more importantly because of their rich and fascinated morphology depending on molecular structure, thermal history, and external stress field.[1–10] The key issue is to establish the relationship between property and morphology, to modulate the morphology of blends and improve the property as much as possible.

In recent years, oscillating shear stress field has been found a very important way to control polymer morphology and mechanical properties. The pioneered work on oscillating packing injection molding went back to 1986, when Prof. Bevis reported such technology and owned the patents.[11] Since then, many investigations have been done on the self-reinforcement of injection-molded polyolefin by using high injection pressure,[12,13] elongation flow,[14,15] or successive macroscopic shears to a solidifying melt in the mold.[16,17] The control of polymer properties by melt vibration technology was summarized in a recent review by Ibar.[18] A shear stress field can also affect the phase behavior dramatically. Shear-induced LCST (lower critical solution temperature) depression and elevation have been observed in several systems.[19–22] It was suggested that shear induces phase separation at low shear rates and depresses LCST but at a phase dissolution at a higher shear rate.[23] The effect of shear fields on phase behavior is theoretically interpreted in terms of the enhancement of concentration fluctuations and the elastic contribution to the free energy of mixing.

It has been well established that HDPE and PP are highly immiscible in the whole range of composition.[24–28] They were found phase separated in the melt state and form separated crystallites (or spherulites) during cooling. However, in a study of PP/HDPE blends, Inoue and coworkers proposed a single-phase mixture of PP/HDPE = 60/40 obtained in high shear fields in an injection machine based on the regularly phase-separated structure.[29]

It now looks interesting to check the miscibility, morphology, and mechanical properties of polymer blends in a high shear rate combined with oscillating shear field during cooling. We carried out experiments for HDPE/PP blends via oscillating packing injection molding after subjecting a high shear rate at the nozzle. A great enhancement of tensile strength was achieved for the blends with PP content less than 10 wt %. The detailed crystal morphologies were investigated by DSC and SAXS.

EXPERIMENTAL

Materials

Polypropylene used in the study was iPP 1250 produced by South Korea, with a melt flow index (MFI) of 1.6 g/min. Polyethylene was HDPE 7006A produced by Qilu Petrochemical Corp., with a MFI of 6.8 g/min.

Samples preparation

Melt blending of HDPE/PP was conducted using twin-screw extruder (TSSJ-25 corotating twin-screw extruder). After making droplets, the blends were molded by oscillating packing injection molding. The schematic representation of dynamic packing molding is shown in Figure 1 and the specimen dimension is shown in Figure 2. The detailed experiment procedures were described in ref. 30. The main feature of this technology is that the specimen is forced to move repeatedly in the mold by two pistons that move reversibly with the same frequency during cooling. We also carried out injection molding under static packing by using the same processing parameters for comparison purpose.

### Mechanical properties measurement

A Shimadzu AG-10TA Universal Testing Machine was used to measure the tensile strength; moving speed was 50 mm/min, and the measure temperature was 20°C.

DSC characterization

The melting behavior was studied by differential scanning calorimetry using Perkin-Elmer DSC priys-1. The instrument was calibrated using indium as the standard. Melting endotherms were obtained at 10°C/min in 4–5 mg of sample. The degrees of crystallinity were calculated from heat of fusion using 293 J/g as the heat of fusion of 100% crystalline polyethylene and 207 J/g for the heat of fusion of pure Polypropylene crystal.[31]
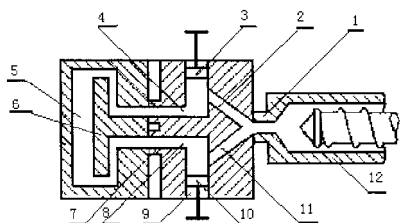
Figure 1 The schematic representation of dynamic packing injection molding. (1) nozzle, (2) sprue A, (3) piston A, (4) runner A, (5) specimen, (6) cavity, (7) connector, (8) runner B, (9) dynamic packing hole, (10) piston B, (11) sprue B, (12) barrel.
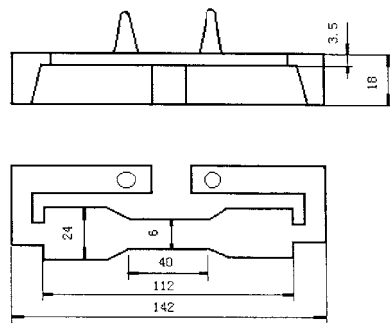
Figure 2 The sketch of mechanical test specimen dimensions according to ASTM638 M standard.

SAXS characterization

The SAXS experiments were carried out with the aid of a Kratky-camera attached to a conventional Cu-K X-ray source, employing a temperature-controlled sample-holder. Scattering curves were usually registered within ten minutes counting time, with the help of a position-sensitive metal wire detector. The slit-smeared data were deconvolved by application of an algorithm developed by Prof. Strobl.[32] The evaluation of the SAXS patterns was carried out assuming that the stacked lamellae have large lateral dimensions. Then it was possible to derive information on the one-dimensional electron density variation $\rho_e(z)$ along the direction normal to the lamellar surfaces. Scattering intensities can be related to the associated electron density correlation function $K(z)$, defined as

$$K(z) = \langle(\rho_e(z) - \langle\rho_e\rangle)(\rho_e(0) - \langle\rho_e\rangle)\rangle$$
$$= \langle\rho_e(z)\rho_e(0)\rangle - \langle\rho_e\rangle^2 \quad (1)$$

and its second derivative $K''(z)$, which gives the interface distance distribution function

$$K''(z) = \frac{O_{ac}}{2} \Delta\rho_e^2[h_a(z) + h_c^i(z) - 2h_{ac}(z)\ldots] \quad (2)$$

where h_a, h_c, and h_{ac} denote the distributions of the thickness of the amorphous and the crystalline layers, and of the long spacings, respectively; O_{ac} is the specific internal surface, i.e., the area per unit volume of the interface separating crystalline and amorphous regions. $\Delta\rho_e$ is the difference of the electron densities of the crystal and the amorphous phase. Both $K(z)$ and $K''(z)$ can be directly calculated by applying Fourier transformations on the scattering intensity distribution $\Sigma(q)$.

For two-phase systems the asymptotic behavior of $\Sigma(q)$ can be described by Porod's law.

$$\lim_{q\to\infty} \sum(q) = r_e^2 \frac{P}{(q/2\pi)^4} \quad (3)$$
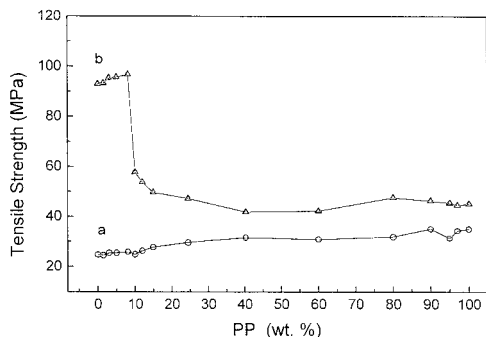
Figure 3 Tensile strength of HDPE/PP blends as a function of composition, (a) obtained by static packing injection molding, and (b) obtained oscillating packing injection molding.

The Porod coefficient P is directly related to O_{ac} by

$$P = \frac{1}{8\pi^3} O_{ac} \Delta p_e^2 \qquad (4)$$

where P shows also up in the slope of the triangular part of $K(z)$, as

$$P = \frac{1}{4\pi^3} \frac{dK}{dz} \qquad (5)$$

RESULTS AND DISCUSSION

Mechanical properties

The tensile strength of blends of HDPE/PP obtained by oscillating packing injection molding is shown in Figure 3. As a function of composition, the tensile strength obtained by static packing injection molding is also included for comparison. One observes a great enhancement of tensile strength of HDPE from 24.7 MPa, by static packing injection molding to 95 MPa by oscillating packing injection molding. The addition of small amount of PP does not cause any change of tensile strength. There exists a sharp decrease of tensile strength as PP content is more than 10 wt %, from 97 MPa (HDPE/PP = 90/10) to 55 MPa (HDPE/PP = 90/15), and then the tensile strength almost keeps constant from 15 wt % of PP to 100 wt % PP. Molecular architecture and phase behavior play an important role in chain orientation; hence, the tensile strength. For HDPE, which has a linear structure, the highest enhancement of tensile strength is obtained. On the other hand, for PP, having a methyl group attached on the backbone, less enhancement is seen. The tensile strength obtained by static packing injection molding can be roughly described by additive law, in agreement with the results in other polyolefin blend systems.[33] It has been well established that HDPE is not miscible with PP, and is phase separated in the liquid state in almost the whole range of composition. This


Figure 4 Core, oriented zone, and skin layer illustrated in the cross-section areas of the samples.

result indicates again that the additive law is not sensitive to phase behavior for samples obtained by static packing injection molding, where not much orientation is expected. However, when the molecular orientation is induced in the sample via oscillating packing injection molding, not only the enhancement of tensile strength is achieved, but also the additive law is broken down. A number of possibilities exist as to why the additive law does not hold true for the samples produced by oscillating packing injection molding. It could be that the molecular response to shear stress field changes as a function of composition. Most likely it could be due to the shear-induced morphology changes. The shear-induced morphologies with core in the center, oriented zone surrounding the core, and skin layer are observed in the cross-section areas of the samples, as shown in Figure 4. The area of oriented zone changes as function of PP content and Figure 5 presents the result. Interestingly, a sharp decrease of oriented zone is seen when PP content is more than 10 wt %, associated with the sharp decrease of tensile strength. This result clearly indicates that oriented zone plays a key role in the enhancement of tensile strength.
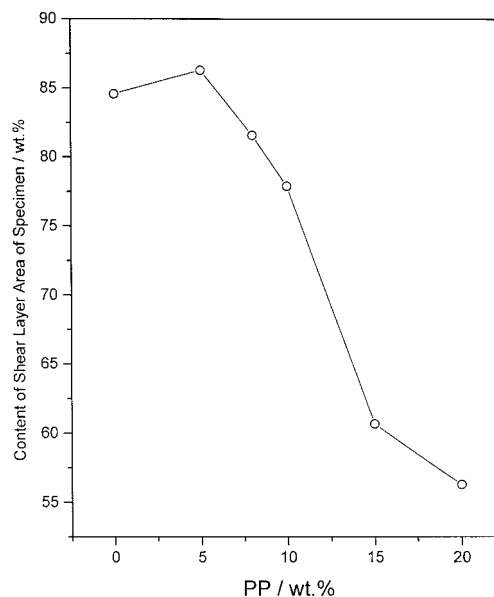
Figure 5 The area of oriented zone changes as a function of composition.
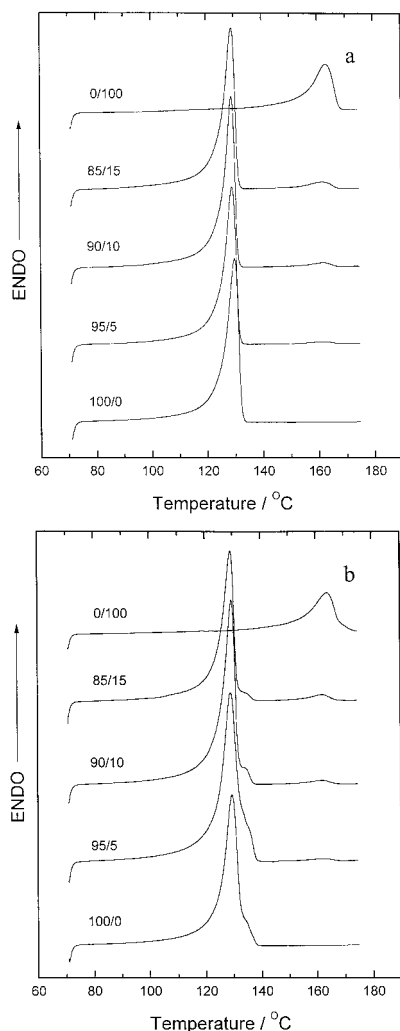
Figure 6 Melting point of HDPE in the blends as a function of composition, (a) obtained by static packing injection molding, and (b) obtained oscillating packing injection molding.

Melting behavior

To understand the dependencies of enhancement of mechanical properties from the point of view of crystal structure, we carried out DSC melting experimental for some samples obtained both by oscillating packing injection molding and static packing injection molding. The result is shown in Figure 6. For samples obtained by static packing injection molding, one melting peak is seen for pure HDPE and PP. And two peaks are seen for the blends, with each of them corresponding to the melting of HDPE and PP, respectively. For samples obtained by oscillating packing injection molding, however, double peaks for HDPE are seen for pure HDPE [Fig. 6(b)], with a high-temperature melting peak that is not present in the endotherms obtained either from the central core or from the samples by static packing injection molding [Fig. 6(a)]. Double melting peaks indicate the existence of shish-kebab structure in the these samples (in the oriented zone).The intensity of high-temperature peak

decreases and gradually disappears with PP content at 15 wt %, which corresponds to the decrease of tensile strength. There is no clear evidence that the blends subject to a large phase separation under the shear rate used, because the heat of fusion of HDPE and PP keeps constant both in the core and the oriented zone before and after oscillating packing injection molding. The crystallinity of HDPE as a function of composition is shown in Figure 7. One observes a linear relationship between crystallinity and composition, and crysatllinity is almost the same for both oscillating samples and static samples at every composition. This result indicates that the enhancement of tensile strength is not due to a change of crystallinity before and after applying the oscillating shear stress to the samples.

SAXS result

There are three possible morphologies for HDPE/PP blends: (1) they are cocrystallized together to form the same lamellae, (2) to form different lamellae but the same spherulite, and (3) to form different spherulite. In our case, no indication is seen for cocrystallization between HDPE and PP. So the morphology should be (2), (3), or a mixture of the two morphologies. The complicated morphology often makes SAXS data analysis very difficult. Even more, one may expect different lamellae thickness for the structure with core and oriented zone of samples obtained by oscillating packing injection molding, which makes impossible the assignment of SAXS peaks. To simplify the SAXS data analysis, we used blends with very small PP content (say 5 w t%); in this case, PP crystal can be neglected, and SAXS data can be consider to represent crystal morphology of HDPE only. Another prerequest for SAXS data analysis is that the crystal morphology is assumed the same in the core and in the oriented zone in microscopy, even in the fact that they are quite
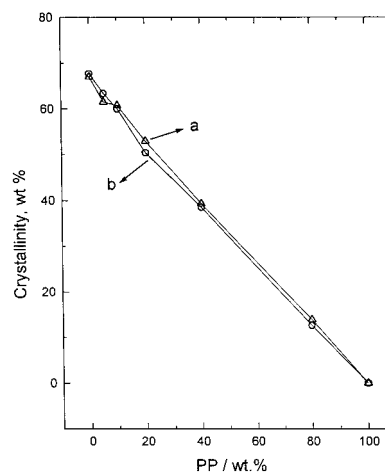
Figure 7 Crystallinity change of HDPE in the blends as a function of composition, (a) obtained by static packing injection molding, and (b) obtained oscillating packing injection molding.

TABLE I
Long Spacing(L), Amorphous Layer Thickness (da), and Crystal Thickness
of Some Samples Obtained by Both Oscillating Packing Injection Molding
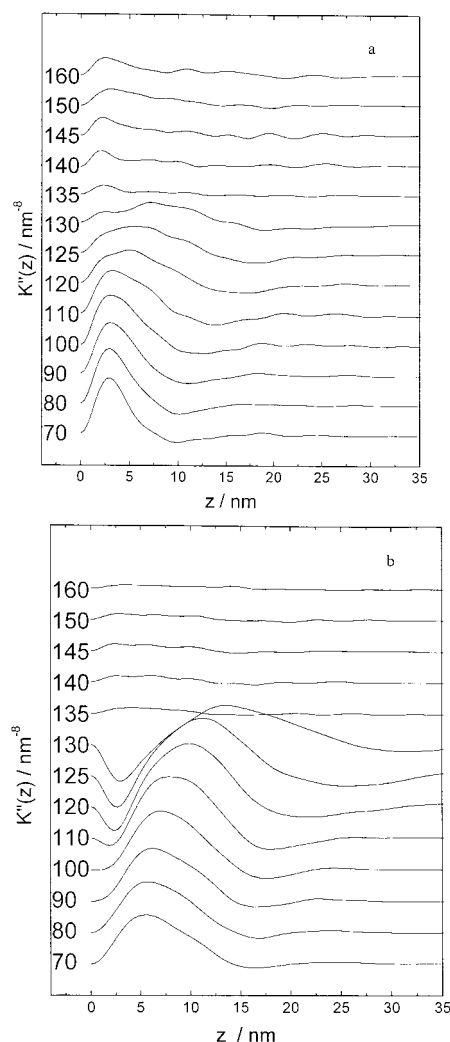**and Static Packing Injection Molding**

HDPE/PP	Oscillating Packing			Static Packing		
	L	da	dc	L	da	dc
100/0	17.2	3.8	13.4	9.9	2.7	7.2
95/5	16.3	5.4	10.9	10.1	3.0	7.1
0/100	17.0	4.3	12.7	12.9	3.1	9.8

different in macroscopic. We carried out SAXS experiment and data analysis with above considerations, and the resulting data looks reasonable as follows.

For SAXS data analysis, we are particularly interested in the interface distance distribution $K''(z)$, from which one can get the most probable thickness of the crystals and amorphous layers. Two peaks (one is for crystal thickness and one is for amorphous layers) and a minimum corresponding to long spacing are seen for all the samples. The peak assignment is based on the DSC data, which shows crystallinity is around 70%. Table I gives data obtained both by oscillating packing injection molding and static packing injection molding. Again, a pure HDPE sample, HDPE/PP = 95/5 sample, and pure PP are chosen as examples, and represent different cases.

From Table I, one can see a big increase of crystals thickness (hc) for samples obtained by oscillating packing injection molding, for examples, from 7.2 to 13.4 nm for HDPE, from 7.1 to 10.9 nm for HDPE/PP = 95/5, and 9.8 to 12.7 nm for PP. One also observes a big increase of amorphous layer thickness (ha) from 3.0 to 5.4 nm for HDPE/PP = 95/5, and only a moderate increase of amorphous layer thickness is seen for HDPE and PP samples. The big increase of ha for HDPE/PP = 95/5 obtained by oscillating packing injection molding, indicates an enhanced miscibility between HDPE and PP under shear stress. In this case, the small amount of PP is most likely located between lamellae of HDPE. A linear crystallinity (ϕ) can be calculated as dc/L = 0.78 for oscillating HDPE and 0.73 for static HDPE, in good agreement with DSC data. Similarly, for HDPE/PP = 95/5, ϕ is calculated as 0.67 (oscillating sample) and 0.70 (static sample), again in agreement with DSC data. Figure 8 shows the evolution of the interface distance distribution function during heating for the HDPE/PP = 95/5 sample, on the left obtained by static packing injection molding and the right-hand side obtained by oscillating packing injection molding. Figure 9 gives the simultaneous changes of the Porod coefficient during heating. At the beginning, one observes an increase in P, as expected due to the increasing electron density difference with temperature. From a certain temperature increase, P decreases, which indicates a melting, and simultaneously a shift of DC is seen in Figure 8. For both samples the decrease in P and the shifting of dc

occurs at 110°C. There may exist a melting recrystallization process above 110°C, as indicated by a step-like increase of DC. For the sample obtained by oscillating packing injection molding, the complete disappearance of $K''(z)$ is seen between 130 and 135°C, and P drops to zero. No crystal structure for PP is observed up to 165°C. It is clearly indicated that crystallization of PP is suppressed, as expected, due to the enhanced

Figure 8 Evolution of the interface distance distribution function $K''(z)$ for HDPE/PP = 95/5 during heating, (a) obtained by static packing injection molding, and (b) obtained oscillating packing injection molding.
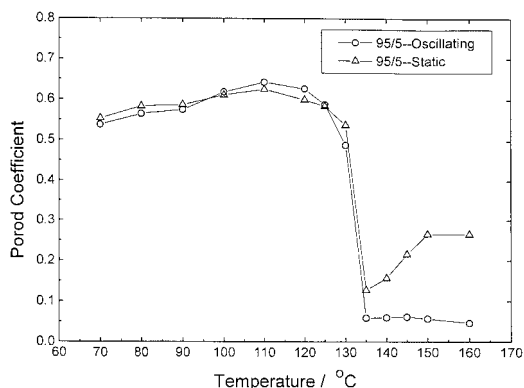
Figure 9 Related changes of the Porod coefficient associated with Figure 5.

miscibility between HDPE and PP induced by shear stress. For the sample obtained by static packing injection molding, however, after complete melting of HDPE, a small peak is seen to show up, and simultaneously an increase in P again is observed, which indicates that PP is phase separated from HDPE and forms crystal lamellar itself. The complete disappearance of the small peak occurs around 160–165°C, corresponding to the final melting of PP, in agreement with DSC data.

So it can be concluded from SAXS data that hat the crystal thickness could be greatly increased under shear stress, and HDPE and PP may form different lamellae but in the same spherulite due to the enhanced miscibility induced by oscillating shear stress. They probably form different spherulites by static packing injection molding.

CONCLUSION

In summary, oscillating stress field can be used as a powerful way to control the property and morphology of polyolefin blends. We have achieved a great enhancement of tensile strength for HDPE and HDPE/PP blends with PP content less than 10 wt % by this method. The additive law can be used, and is not sensitive to phase behavior for samples obtained by static packing injection molding, where not much orientation is expected. However, for samples obtained by oscillating packing injection molding, the additive law is broken down due to complicated morphology composed of molecular orientation and phase separation. Crystallization under shear stress field, the melting point, and crystals thickness of HDPE is greatly improved, and crystallization of PP is suppressed when a small amount PP is mixed with HDPE. DSC and SAXS results suggest a shear-induced miscible between and PP when PP content is less than 10 wt

%, which may result in forming different lamellae but in the same spherulite. The possible crystal morphologies induced by oscillating shear stress are preliminarily investigated by SAXS, and more work is need by AFM and TEM to get the detail morphological information.

REFERENCES

1. Alamo, R. G.; Londono, J. D.; Mandelkern, L.; Stehling, F. C.; Wignall, G. D. Macromolecules 1994, 27, 411.
2. Alamo, R.G.; Graessley, W. W.; Krishnamoorti, R.; Lohse, D. J.; Londono, J. D.; Mandelkern, L.; Stehling, F. C.; Wignall, G. D. Macromolecules 1977, 30, 561.
3. Wignall, G. D.; Alamo, R. G.; Londono J. D.; Mandelkern, L.; Kim, M. H.; Lin, J. S.; Brown, G. M. Macromolecules 2000, 33, 551.
4. Mewis J.; Vinckier I.; Moldenaers, P Macromol Symp 2000, 158, 29.
5. Liu, Y.; Truss, R. W. J Appl Polym Sci 1996, 60, 1461.
6. Minick, J.; Moet, A.; Baer, E. Polymer 1995, 36, 1923.
7. Yu, L.; Shanks, R. A.; Stachurski, Z. H. J Mater Sci Lett 1996, 15, 610.
8. Shanks, R. A.; Li, J.; Yu, L. Polymer 2000, 41, 2133.
9. Hill, M. J.; Barham, P. J.; Keller, A. Polymer 1992, 33, 2530.
10. Hill, M. J.; Barham, P. J. Polymer 1994, 35, 1802.
11. Allen, P. S.; Beivis, M. J. U.K. Pat. 2,170,140B; Eur. Pat. EP0,188,120B1; U.S. Pat. 4,925,161 (1986).
12. Barton, J.; Rak, J. J Appl Polym Sci 1967, 11, 499.
13. Prox, M.; Ehrenstein, G. W. Kunststoffe 1991,81, 1057.
14. Bayer, R. K.; Zachmann, H. G.; Batta Calleja, F. J.; Umbach, H. Polym Eng Sci 1989, 29, 186.
15. Lopez Cabarcos, E.; Bayer, R. K.; Zachmann, H. G.; Balta Calleja, F. J.; Meins, W. Polym Eng Sci 1989, 29, 193.
16. Kalay, G.; Bevis, M. J. J Polym Sci Polym Phys Ed 1995, 55, 1797.
17. Kalay, G.; Allan, P. S.; Bevis, M. J Plast Rubber Compos Process Applic 1995, 23, 71.
18. Ibar, J. P. Polym Eng Sci 1998, 38, 1.
19. Cheith Larbe, F. B.; Malone, M. F.; Winter, H. H.; Halary, J. L.; Leviet, M. H.; Monnerie, L. Macromolecules 1988, 21, 3532.
20. Katsaros, J. D.; Malone, M. F.; Winter, H. H. Polym Eng Sci 1989, 29, 1434.
21. Rectpr, L. P.; Mazich, K. A.; Carr, S. H. J Macromol Sci Phys 1988, B27, 421.
22. Lyngaae-Jorgensen,. J.; Sondergaard, K. Polym Eng Sci 1987, 27, 344.
23. Hindawi, I. A.; Higgins, J. S.; Weiss, R. A. Polymer 1992, 33, 2522; Rudin, A. J Appl Polym Sci 1995, 58, 995.
24. Blom, P. H.; The, J. W.; Rudin, A. J Appl Polym Sci 1996, 60, 1405.
25. Noel, O. F., III; Carley, J. F. Polym Eng Sci 1984, 24, 26.
26. Lovinger, A. J.; Williams, M. L. J Appl Polym Sci 1980, 25, 1703.
27. Djurner, K.; Kubat, J.; Rigdahl, M. Polymer 1977 18, 1968.
28. Bohn, L. Rubber Chem Technol 1968, 41, 495.
29. Sano, H.; Yui, H.; Li, H.; Inoue, T. Polymer, 1998, 39, 5265.
30. Guan, Q.; Shen, K.; Li, J.; Zhu, J. J Appl Polym Sci 1995, 55, 1797.
31. Wunderlich, B. Thermal Analysis; Academic Press: New York, 1990.
32. Strobl, G. Acta Crystallogr 1970, A26, 367.
33. Wang, Y.; Zhang, G.; Chen, L.; Shen K.; Fu, Q. J Appl Polym Sci, submitted.